https://doi.org/10.29227/IM-2025-01-02-001 *Received: 30 Oct 2024, Accepted: 01 May 2025, Published:01 Sep 2025*

Using Image analysis method to determine the degree of saturation of unsaturated sand

Dr. Viet Nam TO[1], Dr. Minh Tuan PHAM[2], Mr. Gia Thong NGUYEN[3]

[1] Faculty of Geology and Petroleum Engineering, Ho Chi Minh City University of Technology, Vietnam National University, Ho Chi Minh City, Vietnam
[2] Faculty of Geology and Petroleum Engineering, Ho Chi Minh City University of Technology, Vietnam National University, Ho Chi Minh City, Vietnam
[3] Faculty of Geology and Petroleum Engineering, Ho Chi Minh City University of Technology, Vietnam National University, Ho Chi Minh City, Vietnam
[*] *Corresponding email: tovietnam@hcmut.edu.vn*

Abstract: *The hydraulic properties of unsaturated soil provide important information on fluid movement in geological systems. The degree of saturation of unsaturated soil, recognized as one of the most critical hydraulic properties, is crucial for geotechnical problems such as slope stability, bearing capacity, and seepage. Computer vision for digital image processing approaches has been widely used recently, with applications in many aspects of construction and geotechnical engineering. The objective of this research is to use the digital image processing (DIP) method to determine the degree of saturation of unsaturated sand. The RGB image of the soil column is processed into a grayscale channel and becomes a matrix for processing calculation. The fluctuation of pixel values extracted from computer vision is correlated with the change in the degree of saturation of the sand. Hence, DIP techniques can be considered as an effective tool to establish the soil-water characteristic curve (SWCC) of unsaturated soil. Furthermore, employing matrix processing techniques can help improve the reliability of the SWCC derived from the correlation between image pixel values and the degree of saturation of unsaturated soil by identifying and mitigating the influence of outliers. The results demonstrate a strong correlation between the degree of saturation obtained through digital image processing techniques and the measured values from resistivity probe techniques.*
Keywords: *DIP, degree of saturation, matrix processing, computer vision, SWCC*

1. Introduction

In unsaturated soil mechanics, understanding the degree of saturation is vital for comprehending how soils behave under various moisture conditions. The degree of saturation quantifies the fraction of the soil's pore space that is occupied by water, and this value directly influences the soil's ability to retain and transmit water. Given its importance, the degree of saturation is fundamental to the Soil-Water Characteristic Curve (SWCC), which illustrates the relationship between soil suction and water content (or degree of saturation). The SWCC is a key empirical tool used in several disciplines, including geotechnical engineering, environmental science, and agriculture, to predict soil behavior and assess soil properties under unsaturated conditions (Fredlund & Xing, 1994).

In the past, traditional methods for measuring the degree of saturation, such as gravimetric and tensiometric techniques, while effective, have limitations, particularly when it comes to analyzing heterogeneous soil samples or monitoring dynamic changes in water content (Durner et al., 1999; Fredlund & Fredlund, 2020; Freund & Rahardjo H, 1993; Habasimbi & Nishimura, 2019; Klute, 1972; To et al., 2013, 2023).

In recent years, digital image processing in determining the degree of saturation of soil has become increasingly important due to its ability to provide high-resolution, non-destructive, and comprehensive data. Digital image processing overcomes many of these challenges by enabling real-time, detailed analysis of the soil's internal structure and moisture distribution. The wide scope of computer vision for digital image processing has been developed due to the application and analysis of images obtained by digital

https://doi.org/10.29227/IM-2025-01-02-001 Received: 30 Oct 2024, Accepted: 01 May 2025, Published:01 Sep 2025

cameras (Dongur et al., 2007). A number of the applications of image processing are optical character recognition, color processing, and fault detection, ect. (Dewangan, 2016). In the field of geotechnical, digital image processing has been used for soil classification by Support Vector Machines (SVMs) combined with Grey Level Co-occurrence Matrix (GLCM) for analyzing image texture of soil(AS et al., 2022; Terribile & Fitzpatrick, 1992). Furthermore, DIP gains significant results in the classification of minerals and characteristics of soil thin sections through several color filters.

The main purposes of this research are to: first, dig into the factors of unsaturated soil adopting with the change of spectrum that can be extracted from Digital Image Processing (DIP) (Delp & Buda, 1985; Hodge & Austin, 2004). Soil column samples were photographed at various stages during the one-dimensional drainage process using a digital camera. The captured images were subsequently analyzed through Digital Image Processing (DIP) techniques, which involve processing and extracting relevant information from the images.; second, apply the mean absolute deviation as the filter to remove the heterogeneous factors of soil captured on digital (Konno & Koshizuka, 2005; Mehrang et al., 2015) the color gradient variations observed in the images, which correspond to different moisture levels within the soil. These variations allowed for the quantification of the degree of saturation at each stage of the drainage process. However, the outlier of color gradient still contains and must be migrated from the distribution. Third, measure the degree of saturation of soil by resistivity probe. The degree of saturation obtained from the DIP analysis was then compared with the values measured from a resistivity probe, providing a means of validating the results and evaluating the accuracy of the image-based method. This comparison demonstrates the potential of DIP as a non-invasive, high-resolution technique for assessing the degree of saturation in soil, complementing traditional methods used in geotechnical investigations (Archie, 1942; Lu et al., 2020; Merritt et al., 2016).

2. Geological background

The column of sand is 700mm in height, and the inner area is 200x200mm; the Plexiglas wall has a thickness of 10mm. The sample sand is collected in Tay Ninh province. The properties of the sample include Gs=2.66, Cu=1.65, Cc=0.94; the sand particles have a mean diameter of approximately D50=0.55mm. The process of the vertical drainage test is recorded by the camera that took pictures every 2 minutes during the drainage from the beginning to 24 hours.

3. Methodology

3.1 Data analysis

The soil column image is captured by a camera, which is illustrated by a red, green, and blue color system (RGB). The RGB color system works by combining different amounts of three primary colors (red, green, blue) to create a wide range of colors. The combination can be dedicated to each pixel in the form of a matrix [x, y, z], where x, y, z are the values of red, green, and blue intensities, respectively. The color intensity of each is represented by a range of values from 0 to 255. This matrix type is dedicated to W in this issue:

$$W = [x\ y\ z\ ] \qquad \text{(Eq.1)}$$

The image that needs to be processed can be represented by this type of matrix:

$$\text{IMG}=\begin{bmatrix} W_{1.1} & W_{1.2} & \dots & W_{1.m} \\ W_{2.1} & \dots & \dots & \dots \\ \dots & \dots & \dots & \dots \\ W_{n.1} & \dots & \dots & \dots \end{bmatrix} \qquad \text{(Eq.2)}$$

Where m and n are the number of rows and columns of pixels, each value of W has the dimension of 3 columns, so that the shape of the IMG matrix is implied as (m, n,3).

The changes of soil saturation degree to the height of the soil column can be observed visibly in Fig.1. Then, these changes are extracted and executed to become well fit with the measured data using a resistivity probe.

https://doi.org/10.29227/IM-2025-01-02-001 Received: 30 Oct 2024, Accepted: 01 May 2025, Published:01 Sep 2025

3.2 Computer vision

Fig.1c shows the result of the vertical drainage test after 24h, when the change of degree of saturation in the soil column is small. In the first step, this image would be worked on to be the optimal size and shape for further calculation. Then, the range of values that are used for indicating saturated, transition, and unsaturated zones should be determined by the brightness of pixels. Following zone classification, assign saturation values to each class based on the corresponding brightness levels using boundary condition interpolation. Then, visualize the relationship between the obtained saturation values and soil suction to illustrate the SWCC. Identifying the territory of values that are impacted by external factors that make the parameters not fit well with SWCC. Noise is reduced by applying the Mean Absolute Deviation (MAD) filtering method, and the final results are validated against laboratory data.

In addition, the DIP method needs to be evaluated by a more realistic experiment. So, a measurement is executed in the laboratory for the same column sample. The principle of this measurement involves using a probe to obtain the change of soil saturation with the soil column height.

https://doi.org/10.29227/IM-2025-01-02-001 Received: 30 Oct 2024, Accepted: 01 May 2025, Published:01 Sep 2025

(a) (b) (c)

Fig.1. Vertical drainage test with soil column **(**a) At the beginning, (b) After 5 minutes, (c) After 24h.

3.2.1 Digital Image Processing

The soil column used in this research has 700mm in height, the Fig.1c should be divided into the number of pixel arrays, which is the divisor of 700. In other words, the picture is executed as a matrix that has 2100 rows and 567 columns.

Based on Eq.2, Fig.1c can be converted to the matrix with the formula below:

$$\text{IMG1}=\begin{bmatrix} W_{1.1} & W_{1.2} & \dots & W_{1.567} \\ W_{2.1} & \dots & \dots & \dots \\ \dots & \dots & \dots & \dots \\ W_{2100.1} & \dots & \dots & \dots \end{bmatrix} \qquad \text{(Eq.3)}$$

IMG1 has the matrix dimension (2100,567,3) with 2100 rows, 567 columns, and each pixel has dimension (3,1). This shape of matrix makes it difficult for further processing because it is very complex to deal with a multi-layer matrix calculation. So, Fig.1c should be converted from a 3-channel color system (RGB system) into a 1-channel color system, such as grayscale color. The formula to convert is:

$$A = \sqrt{x_w + y_w + z_w} \qquad \text{(Eq.4)}$$

where:

A: Grayscale color can be considered as brightness of pixels

x_w ,y_w, z_w: Color intensity of Eq.1

Fig.1c after the process through Eq.4 should be the new matrix below:

$$\text{IMG2}=\begin{bmatrix} A_{1.1} & A_{1.2} & \dots & A_{1.567} \\ A_{2.1} & \dots & \dots & \dots \\ \dots & \dots & \dots & \dots \\ A_{2100.1} & \dots & \dots & \dots \end{bmatrix} \qquad \text{(Eq.5)}$$

The new matrix IMG2 has the shape (2100,567) due to conversion from Eq.4; values of A have a range from 0 to 255. IMG2 becomes easier to extract due to the fact that it can be solved by matrix processing.

3.2.2 Arrangement of pixel's values

Fig.2 shows the distribution of different brightnesses of the soil column. There are 3 distinguished parts that can be determined due to their brightness. These different zones can be considered as light zone (1), transient zone (2), and dark zone (3) (Fig.3)

It is a critical task to find which brightness value represents each zone exhibited above because each soil layer would have different saturation with respect to soil suction. In other words, the matrix IMG2 should be divided into smaller submatrices with respect to the height of the soil column. IMG2 can be separated into 30 submatrices, each standing for 10mm from 2100 rows of pixels for 700mm. The shape of each submatrix is (30,567).

In order to demonstrate the difference in brightness from the observation to the value that can be used to calculate. We should indicate them as the percentage of light pixels on each layer. Light pixels could be determined by comparing the number of values that are the majority in the light zone and the minority in the dark zone.

The distribution of whole pixel values has the most population in the range from 100 to 180 (Fig.4). It is the majority of values in the range of 135 to 185 in the light zone Fig.6; otherwise, these values are not well populated in the dark zone so the range of 135 to 185 should be considered to be used as values for light pixels.

3.2.3 Indicating pixels by brightness and interpolating them with saturation values.

In this study, the range of light brightness is determined by visualizing a histogram. This parameter is essential for determining the percentage of light pixels in each layer. The percentage of light pixels in each layer can be calculated by:

https://doi.org/10.29227/IM-2025-01-02-001 *Received: 30 Oct 2024, Accepted: 01 May 2025, Published:01 Sep 2025*

$$\%B = \frac{B}{T} \times 100 \qquad \text{(Eq.6)}$$

where:

%B: Percentage of light pixels

B: Number of light pixels

T: Total pixels

https://doi.org/10.29227/IM-2025-01-02-001 Received: 30 Oct 2024, Accepted: 01 May 2025, Published:01 Sep 2025

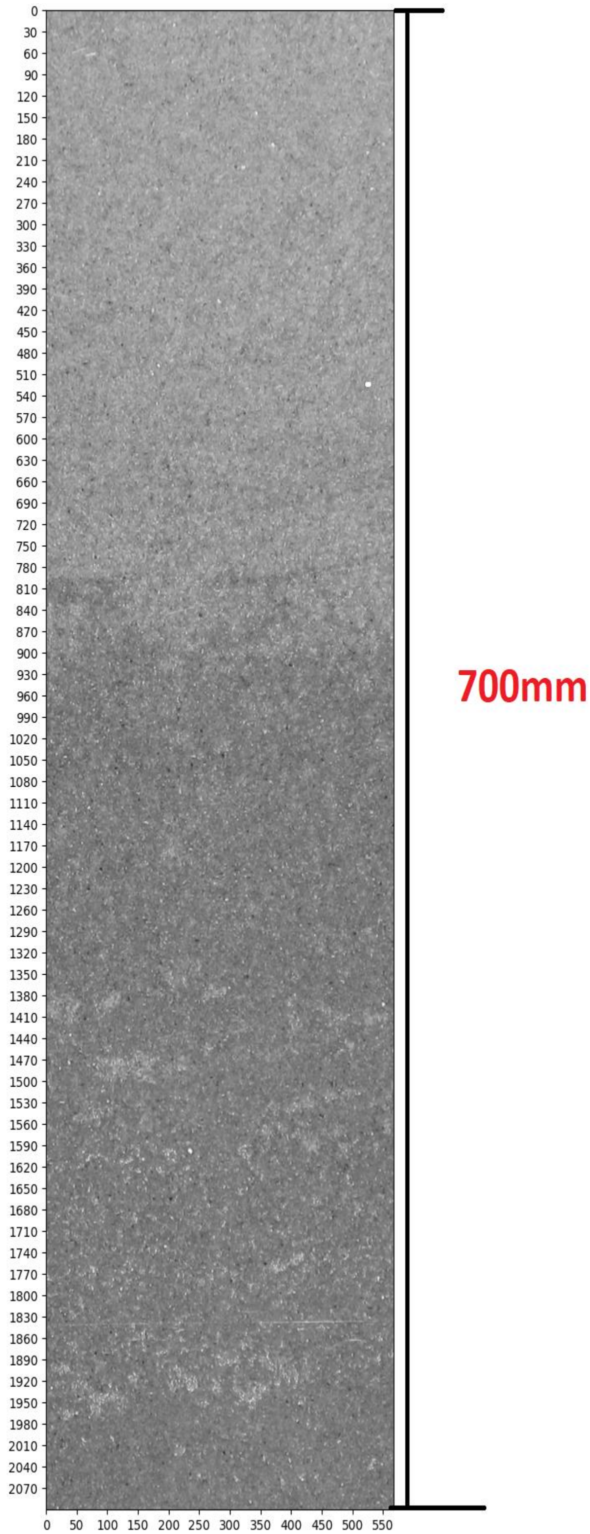

Fig.2. 24h vertical drainage soil column (700mm) after digital image processing.

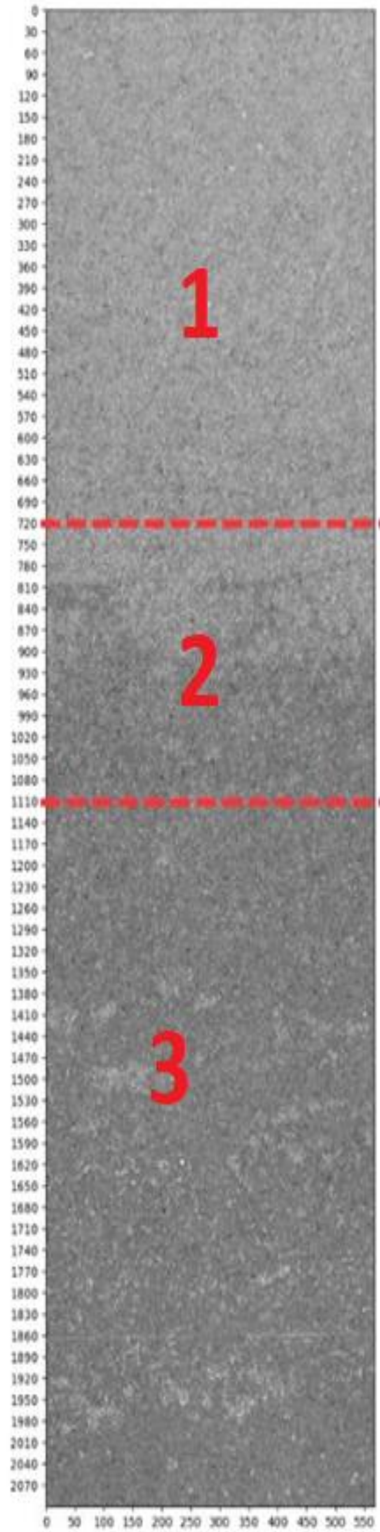

Fig.3. Light zone (1). Transient zone (2). Dark zone (3)

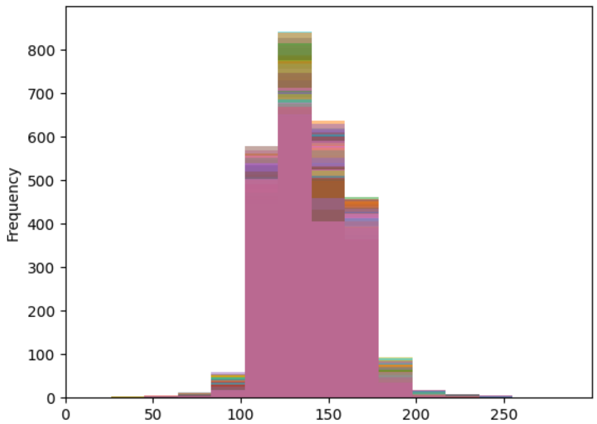

Fig.4. Distribution of pixel values for all three distinguish zones (0-700mm)

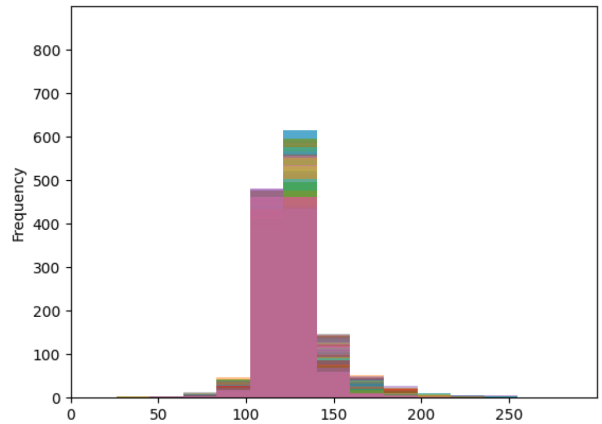

Fig.5. Distribution of pixel values for dark zone (0-340mm)

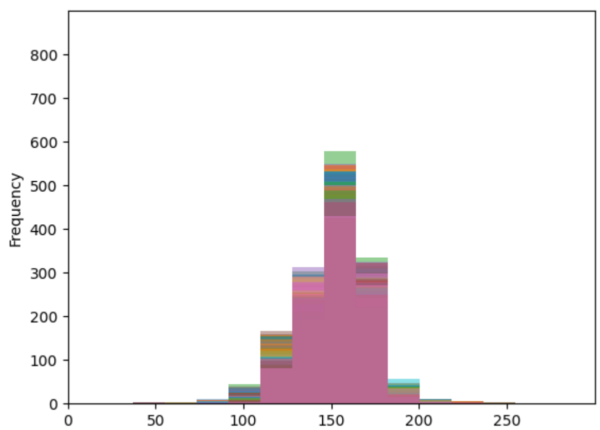

Fig.6. Distribution of pixel values for light zone (470-700mm)

The percentage of light pixels for each submatrix is obtained by applying Eq.6 to them, which could be considered as the saturation values at certain locations. Where the %B has a low value, it means that the value of soil saturation of this location is very high. According to this principle, the saturation value can be calculated by the boundary condition interpolation method.

Boundary condition for soil saturation-percentage of light pixels interpolation:

$$S = \left(\frac{\%B - min\%B}{max\%B - min\%B}\right) * (maxS - minS) + minS \qquad \text{(Eq.7)}$$

where:

%B: Percentage of light pixels

S: Soil saturation values

After obtaining soil saturation values, SWCC can be sketched, but the value of saturation values does not fit well with SWCC. Mean Absolute Deviation (MAD) could be used as a filter to control the quality of soil saturation.

3.3 Experiments

3.3.1 The measurement for soil saturation with the soil suction

https://doi.org/10.29227/IM-2025-01-02-001 Received: 30 Oct 2024, Accepted: 01 May 2025, Published:01 Sep 2025

A resistivity investigation tool is developed to determine values of soil saturation due to the change of soil resistivity with the soil suction. The design of a resistivity probe with 2 stainless steel electrodes (D= 2mm), 100mm in length, and a gap between 2 polar equal to 12mm (L). Thirteen pairs of polar probes were distributed along the height of the column. The electrical signal was transmitted through the soil between the gap of two electrical poles of the probes. The transition of electricity current was controlled by the electrical resistivity tester's device (Fig.7). The device was programmed to allow electric current to flow through a pair of polarities at specific depths, preventing interference between the signals. This configuration ensures that the signals remain clear and free from noise caused by other channels.

As demonstrated by Fig.8, the resistivity probes are used to obtain values of the voltage signal (ΔV) and electric current intensity (I). Utilize the function below to calculate resistivity (R) values:

$$R = \frac{\Delta V}{I} \qquad \text{(Eq.8)}$$

where:

R: Resistivity of soil (Ω)

ΔV: Voltage signal variation (V)

I: Electricity current intensity (A)

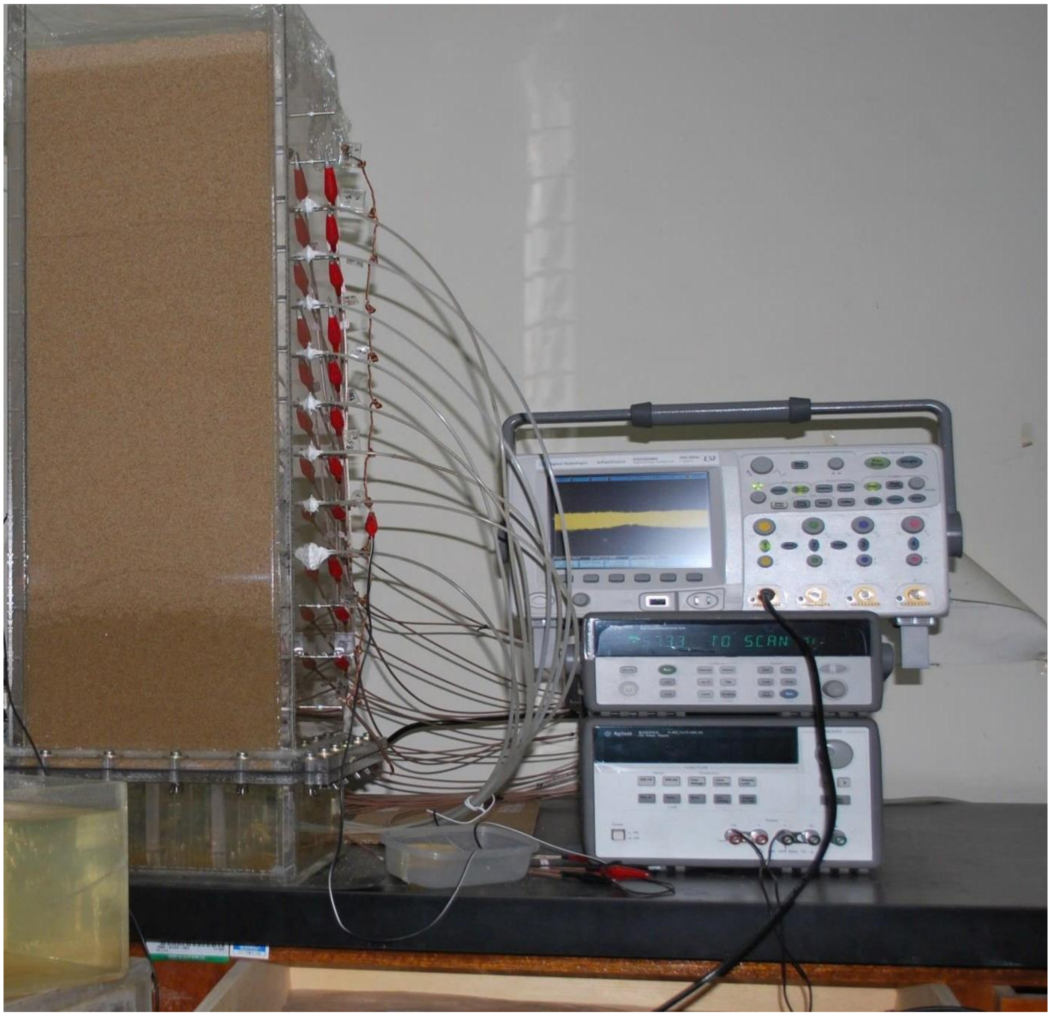

Fig.7. Electrical resistivity testers for resistivity probe

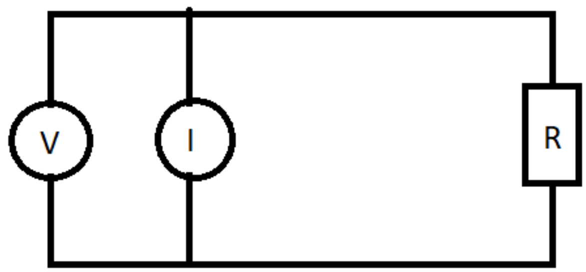

Fig.8. Prototype of resistivity probes to obtain electricity parameters (U and I)

Water saturation should be determined by the relationship between soil resistivity and water saturation of soil. This relationship is represented by Archie's equation (Archie, 1942):

$$S_w = \left(\frac{\rho_w \Phi^{-m}}{\rho_s}\right)^{\frac{1}{n_a}} \quad \text{(Eq.9)}$$

where:

S_w: Water saturation (%)

ρ_w: Density of water (g/cc)

ρ_s: Density of soil (g/cc)

m and n_a : Archie's exponentials

Φ: Soil porosity (%)

The density of soil and water could be determined by the equation:

$$\rho = \frac{RA}{L} \quad \text{(Eq.10)}$$

where:

A: Section of probe (mm2)

L: Gap between 2 polar (mm)

4. Results

4.1 Interpolating pixel value into degree of saturation

The relationship between the percentage of light pixels and soil column height is demonstrated in Fig.9. The Number of light pixels is dominated by darker pixels in the lower area of the soil column. The distribution of dark and light pixels varied from the bottom to the top of the column as an S-shape curve. Generally, most of the light pixels are concentrated at the top of the soil column, while the dark pixels are mainly located at the bottom. The S-shape distribution curve seems to be an inverse curve of SWCC.

According to Fredlund's SWCC equation (Fredlund & Fredlund, 2020), it is divided into 3 vadose zones: the pendular zone, where most of the water is residual, the capillary zone, where the water's degree of saturation at maximum and the last is funicular zone where the transition between unsaturated and saturated zone can be observed. Applying Eq.7 in order to interpolate the distribution of pixels into the distribution of degree of saturation. As seen in Fig.9, the range of the percentage of light pixels (%B) varies from 23% to 96% in this result. Assuming the change of degree of saturation (S) fluctuates from 13% to 100%. Interpolated degree of saturation can be seen in Fig.10; the result nearly fits well with Fredlund's SWCC curve. However, the fluctuation of the degree of saturation at the bottom of the column seems quite chaotic. It could be affected by external factors when conducting experiments or capturing images. So, an adjustment needs to be executed to be fitted with the standard SWCC Curve.

4.2 Quality control for DIP

As considered previously, the range of light pixels is from 135 to 185; similarly, the range of dark pixels should be considered in the range of 100 to 135. Observing the distribution of dark zones in Fig.5, there are invasions of light pixels in the distribution. These invaders can be determined as outliers. The distribution of pixels observed in Figs 1,2,3 seems disorderly, but they gather in a certain range of values. So, this distribution satisfies the requirement for applying Mean Absolute Deviation (MAD) as a filter to remove outliers. The equation of MAD is below:

$$MAD = \frac{\sum_{i=1}^{n}\left|x_i - \underline{x}\right|}{n} \quad \text{(Eq.11)}$$

The purpose of Eq.11 is to reduce as much as possible the outliers caused by external factors. The final results with better data quality are demonstrated in Fig.11. The soil suction increases as the depth of the soil column increases. In this experiment, the maximum soil suction was approximately 5.5 kPa at the bottom of the column. So as to, Fig.11 can be interpolated into Fig.12, which illustrates the relationship between soil suction and degree of saturation of soil.

4.3 Results of resistivity probe measurement.

The shape of the obtained curve from Fig. 13 aligns well with the trends observed in the Soil Water Characteristic Curve (SWCC), demonstrating its suitability for assessing the reliability of the DIP method. Applying regression for variables of SWCC obtained from the resistivity probe measurements and the DIP method, the correlation coefficient (R^2) of them is 95.17%.

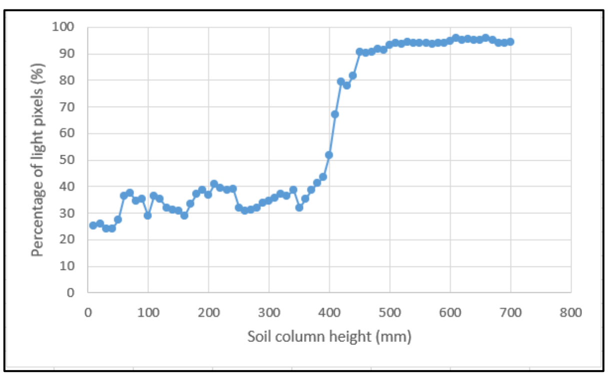

Fig.9. Percentage of light pixels versus column height

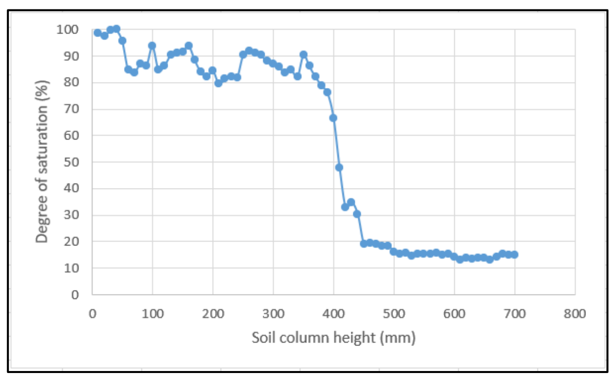

Fig.10. Degree of saturation versus column height

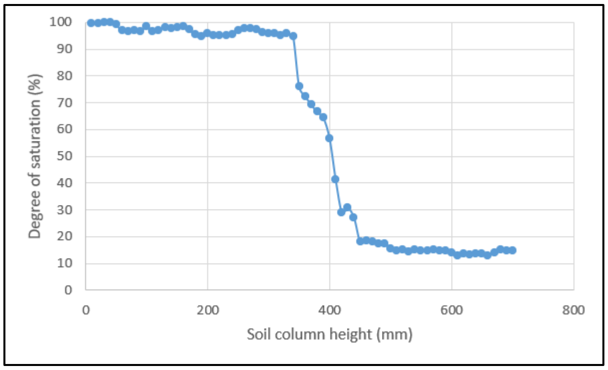

Fig.11. Degree of saturation versus column height after MAD adjustment

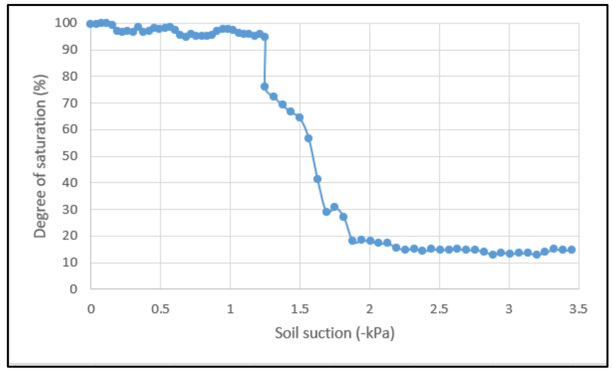

Fig.12. Degree of saturation versus soil suction after MAD adjustment

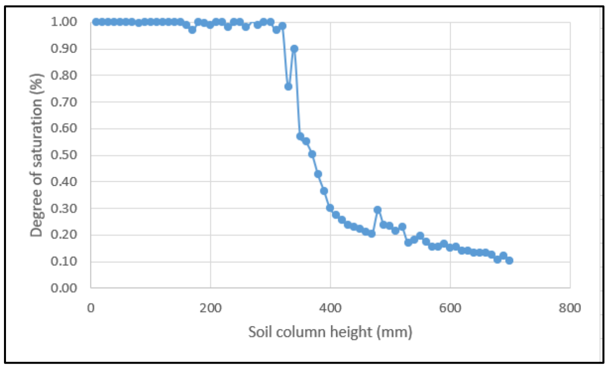

Fig.13. Measured Degree of saturation belong the Soil column

5. Discussion

Both Fig.12 and Fig.13 illustrate the same trend of the relationship between soil suction and the degree of saturation of soil. In Fig.12, the degree of saturation indicates high saturation in dark pixel areas. At the bottom of the column, dark pixels are very dense, with their intensity decreasing as high as the height of the soil column. The distribution of dark pixels begins to decrease significantly in the range of height 350mm to 440mm. From a height of 440mm to the top of the column is dominated by light pixels. On the other hand, the result of resistivity measuring techniques also has the same trend. The distribution of soil saturation from 0 to 320 fluctuates around 100%. There is only 1 abnormality at 220mm, which has a degree of saturation of 69%. This singularity might be caused by the heterogeneity of soil structure, which is affected by the precision of tools. From the height of column 320 to 400 mm, the degree of saturation significantly drops from nearly 100% to 30%. The soil saturation at a height of 470 degrees decreased from 20% to 10%. The change of parameters of both methods has a general pattern, and the style of changing at certain heights seemed to correlate with others. The correlation coefficient of the 2 methods is very high (R2=95.17%). This means that in case only an image database is available, computer vision can be a reliable method to determine the degree of saturation in unsaturated soil in comparison with a conventional method like probe resistivity.

6. Conclusion

The new approach with the DIP method seems suitable for the degree of soil saturation indication problems. Based on the RGB image of the soil column treated by the vertical drainage method. The established DIP model demonstrated its benefit for geologists to determine soil saturation without complex measurement and expensive tools.

The evaluation between experiment results from the resistivity probe and the results from the DIP method shows that the DIP method was effective and could be used to obtain the degree of saturation from the brightness of images. These parameters are used for establishing the relationship between the degree of saturation and soil suction, which is represented by SWCC.

In further research, this is a potential method that can be used to determine the degree of saturation for other soils and materials, which have more complex boundary conditions.

Acknowledgements.

This research is funded by Vietnam National University HoChiMinh City (VNU-HCM) under grant number C2024-20-27

Literatura - References

1. Archie, G. E. (1942). The Electrical Resistivity Log as an Aid in Determining Some Reservoir Characteristics. *Transactions of the AIME*, *146*(01), 54–62. https://doi.org/10.2118/942054-G
2. AS, M., Abdullah, H., Syahputra, H., Benaissa, B., & Harahap, F. (2022, October 11). An Image Processing Techniques Used for Soil Moisture Inspection and Classification. *ICIESC*. https://doi.org/10.4108/eai.11-10-2022.2325509
3. Delp, E. J., & Buda, A. J. (1985). Digital Image Processing. In *Digital Cardiac Imaging*. Martinus Nijhoff.
4. Dewangan, S. K. (2016). Importance and Applications of Digital Image Processing. *International Journal of Computer Science & Engineering Technology*, *7*(07), 2229–3345. http://www.ijcset.com/docs/IJCSET16-07-07-003.pdf
5. Dongur, K. R., Tandekar, P., & Purve, S. K. (2007). Digital Image Processing: Its History and Application. *International Journal of Advanced Research in Computer and Communication Engineering ISO*, *3297*(6), 364–367. https://doi.org/10.17148/IJARCCE.2022.11672
6. Durner, W., Bernd Schultze, & Torsten Zurmühl. (1999). State-of-the-art in inverse modeling of inflow/outflow experiments. *Proceedings of the International Workshop on Characterization and Measurement of the Hydraulic Properties of Unsaturated Porous Media*. https://www.researchgate.net/publication/236901674
7. Fredlund, D. G., & Fredlund, M. D. (2020). Application of 'estimation procedures' in unsaturated soil mechanics. *Geosciences (Switzerland)*, *10*(9), 1–22. https://doi.org/10.3390/geosciences10090364
8. Fredlund, D. G., & Xing, A. (1994). Equations for the soil-water characteristic curve. *Can. Geotech*, *31*, 521–532. www.nrcresearchpress.com
9. Freund, D. G., & Rahardjo H. (1993). *Soil Mechanics for Unsaturated Soils*. John Wiley & Sons, Inc. https://doi.org/https://dx.doi.org/10.1002/9780470172759
10. Habasimbi, P., & Nishimura, T. (2019). Soil Water Characteristic Curve of an Unsaturated Soil under Low Matric Suction Ranges and Different Stress Conditions. *International Journal of Geosciences*, *10*(01), 39–56. https://doi.org/10.4236/ijg.2019.101004
11. Hodge, V., & Austin, J. (2004). A Survey of Outlier Detection Methodologies. *Artificial Intelligence Review*, *22*(2), 85–126. https://doi.org/10.1023/B:AIRE.0000045502.10941.a9
12. Klute, A. (1972). The determination of the hydraulic conductivity and diffusivity of unsaturated soils. *Soil Science*, *113*(4), 264–276. https://doi.org/10.1097/00010694-197204000-00006
13. Konno, H., & Koshizuka, T. (2005). Mean-absolute deviation model. *IIE Transactions*, *37*(10), 893–900. https://doi.org/10.1080/07408170591007786
14. Lu, D., Wang, H., Huang, D., Li, D., & Sun, Y. (2020). Measurement and Estimation of Water Retention Curves Using Electrical Resistivity Data in Porous Media. *Journal of Hydrologic Engineering*, *25*(6). https://doi.org/10.1061/(ASCE)HE.1943-5584.0001925
15. Mehrang, S., Helander, E., Pavel, M., Chieh, A., & Korhonen, I. (2015). Outlier detection in weight time series of connected scales. *2015 IEEE International Conference on Bioinformatics and Biomedicine (BIBM)*, 1489–1496. https://doi.org/10.1109/BIBM.2015.7359896
16. Merritt, A. J., Chambers, J. E., Wilkinson, P. B., West, L. J., Murphy, W., Gunn, D., & Uhlemann, S.

(2016). Measurement and modelling of moisture—electrical resistivity relationship of fine-grained unsaturated soils and electrical anisotropy. *Journal of Applied Geophysics*, *124*, 155–165. https://doi.org/10.1016/j.jappgeo.2015.11.005

17. Terribile, F., & Fitzpatrick, E. A. (1992). The application of multilayer digital image processing techniques to the description of soil thin sections. In *Geoderma* (Vol. 55). https://doi.org/https://dx.doi.org/10.1016/0016-7061(92)90011-U
18. To, N. V., Min, T. K., & Shin, H. (2013). Using inverse analysis to estimate hydraulic properties of unsaturated sand from one-dimensional outflow experiments. *Engineering Geology*, *164*, 163–171. https://doi.org/10.1016/j.enggeo.2013.07.005
19. To, N. V., Nguyen, K. V., Dao, H. H., & Phu, T. N. (2023). Using Inverse Technique to Evaluate the Effect of Capillary Barrier on Hydraulic Properties of Unsaturated Multi-Layered Sand from 1-D Desaturation Test. *Lecture Notes in Civil Engineering*, *268*, 679–688. https://doi.org/10.1007/978-981-19-3303-5_61